REVIEW

Scanning Probe Evolution in Biology

J. K. H. Hörber[1] and M. J. Miles[2]*

Twenty years ago the first scanning probe instrument, the scanning tunneling microscope, opened up new realms for our perception of the world. Atoms that had been abstract entities were now real objects, clearly seen as distinguishable individuals at particular positions in space. A whole family of scanning probe instruments has been developed, extending our sense of touching to the scale of atoms and molecules. Such instruments are especially useful for imaging of biomolecular structures because they can produce topographic images with submolecular resolution in aqueous environments. Instruments with increased imaging rates, lower probe-specimen force interactions, and probe configurations not constrained to planar surfaces are being developed, with the goal of imaging processes at the single-molecule level—not only at surfaces but also within three-dimensional volumes—in real time.

The importance of the development of scanning probe microscopy (SPM) is comparable to that of electron microscopy and even optical microscopy. SPM measures the near-field physical interactions between the scanning probe tip and the atoms that lie beneath it as it moves. Atomic force microscopy (AFM) (*1*), a member of the SPM family, has become particularly important for the study of biological systems. AFM produces three-dimensional (3D) images of a surface at atomic resolution; even subatomic resolution has been reported for atomic orbitals on a silicon surface (*2*). Its major advantage is that it can produce high-resolution topographic images in aqueous and physiologically relevant environments without the need to stain the specimen; the AFM contrast mechanism does not depend on atomic number, but simply senses the specimen surface through the force between it and a sharp probe that scans the surface.

Local probes, the central feature of all scanning probe instruments, are small-sized objects such as the ends of sharp tips; the interaction of the tip with the surface of a sample can be sensed at selected positions. Proximity to or contact with the sample is required for high spatial resolution. The principal idea is quite old and had appeared in literature from time to time, in the context of bringing a source of electromagnetic radiation in close contact with a sample, but was not pursued until recently. Nanoscale local probes require atomically stable tips and high-precision manipulation devices. The latter are based on mechanical deformations of springlike structures by given forces—piezoelectric, mechanical, electrostatic, or magnetic—to ensure continuous and reproducible displacements with precision down to the picometer level. They also require effective acoustic, thermal, and vibration isolation. The resolution that can be achieved with local probes is primarily a function of the effective probe size, its distance from the sample, and the distance dependence of the interaction between probe and sample measured. The last can be considered to create an effective aperture by selecting a small feature of the overall geometry of the probe tip, which then corresponds to the effective probe.

The ability of AFM to yield images under ambient conditions or in solution was considered from the outset to provide an ideal tool for physical studies of biological specimens under physiological conditions. Contact-mode, constant-force AFM imaging could show processes induced by viral infection on live cells (*3*) and has achieved atomic-scale resolution images of cellulose microfibrils (*4*). In recent years, high-resolution AFM imaging has also been achieved on bacterial membrane proteins (*5*). Recently, the analysis of AFM images of 2D crystals of membrane proteins such as aquaporin-Z (Fig. 1) has been developed to the extent that the free energy landscape can be derived for domains within single protein molecules. From the raw AFM data (Fig. 1A), an average topograph for a single protein molecule is calculated (Fig. 1B) with processing techniques more commonly used in transmission electron microscopy. From this, the conformational space of the protein can be derived by calculating the

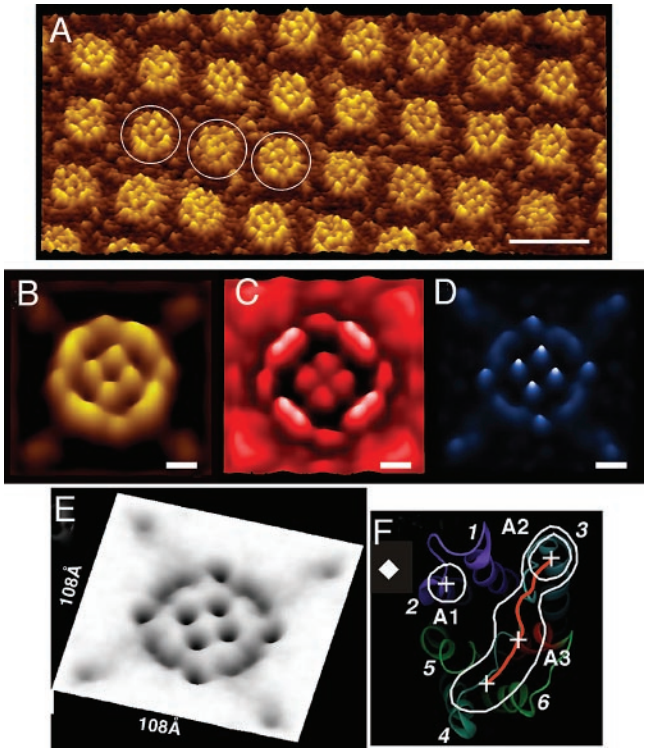

Fig. 1. (**A**) High-resolution raw data AFM image of aquaporin-Z (AqpZ) 2D crystal. The circles indicate individual extracellular protein molecule surfaces. Scale bar, 10 nm; full grayscale, 1 nm. (**B**) Topograph of a single protein from average of 1477 aligned trimers. Scale bar, 1 nm; grayscale range, 0.01 to 0.07 nm. (**C**) Standard deviation map about the averaged structure in (B). (**D**) Probability position map. Scale bar, 1 nm. (**E**) Free energy landscape calculated from (D). (**F**) A monomer of the porin AqpZ atomic model with overlay of the full width at half-maximum outline. Crosses indicate high-probability positions; the red line is the top probability tracing line of loop C. Transmembrane helices are numbered in italics. Helices 1 and 2 are connected by loop A1; helices 3 and 4 are connected by loop A3. Contour A2 corresponds to the protruding end of helix 3 out of the membrane surface. The colors of the helices indicate the pairing to form the loops.

[1]Department of Physiology, Wayne State University School of Medicine, 5229 Scott Hall, 540 East Canfield Avenue, Detroit, MI 48201, USA. [2]H. H. Wills Physics Laboratory, University of Bristol, Tyndall Avenue, Bristol BS8 1TL, UK.

*To whom correspondence should be addressed. E-mail: m.j.miles@bristol.ac.uk

standard deviation from this average structure of all the protein topographs (Fig. 1C). Similarly, the probability distribution of topographic peaks in the protein domains under thermal motion can be calculated (Fig. 1D), and from this the free energy landscape (Fig. 1E) can be derived. A comparison of this landscape can then be correlated with the atomic structure of the protein (Fig. 1F).

In the application of AFM to live cells, the instrument has revealed new cellular structures and their function (e.g., an exocytotic fusion pore). Fusion of membrane-bound secretory vesicles at the cell plasma membrane and consequent expulsion of vesicular contents is a fundamental cellular process regulating neurotransmission, enzyme secretion, and hormone release. Secretory vesicles dock and fuse at defined plasma membrane locations, following secretory stimuli. Electrophysiological studies on single cells suggest the presence of fusion pores at the cell plasma membrane, which become continuous with the secretory vesicle membrane after stimulation of secretion. AFM performed at nanometer resolution on live pancreatic acinar cells by Jena's group (*6*) revealed the presence of the fusion pore at the apical plasma membrane, as well as its structure and dynamics. These studies showed pit-like structures containing typically three or four "depressions," 150 nm in diameter, at the apical plasma membrane in live pancreatic acinar cells. The stimulation of secretion causes these depressions to dilate and to return to their resting size after completing the process. Exposure of acinar cells to the actin depolymerizing agent cytochalasin B results in decreased depression size and a loss in stimulable secretion, a process that can be followed by AFM observation. Zymogen granules, the membrane-bound secretory vesicles in exocrine pancreas, contain the starch-digesting enzyme amylase. Using amylase-specific immunogold labeling together with AFM, Jena's group has also demonstrated localization of amylase at depressions after stimulation of secretion. These experiments confirm depressions to be the fusion pores in pancreatic acinar cells. Further studies in several laboratories reveal the presence of similar fusion pores in neuroendocrine cells. Fusion pores are the first cellular structures to have been identified by AFM as permanent structures at the cell plasma membrane of secretory cells, where membrane-bound secretory vesicles dock and fuse to release vesicular contents (Fig. 2).

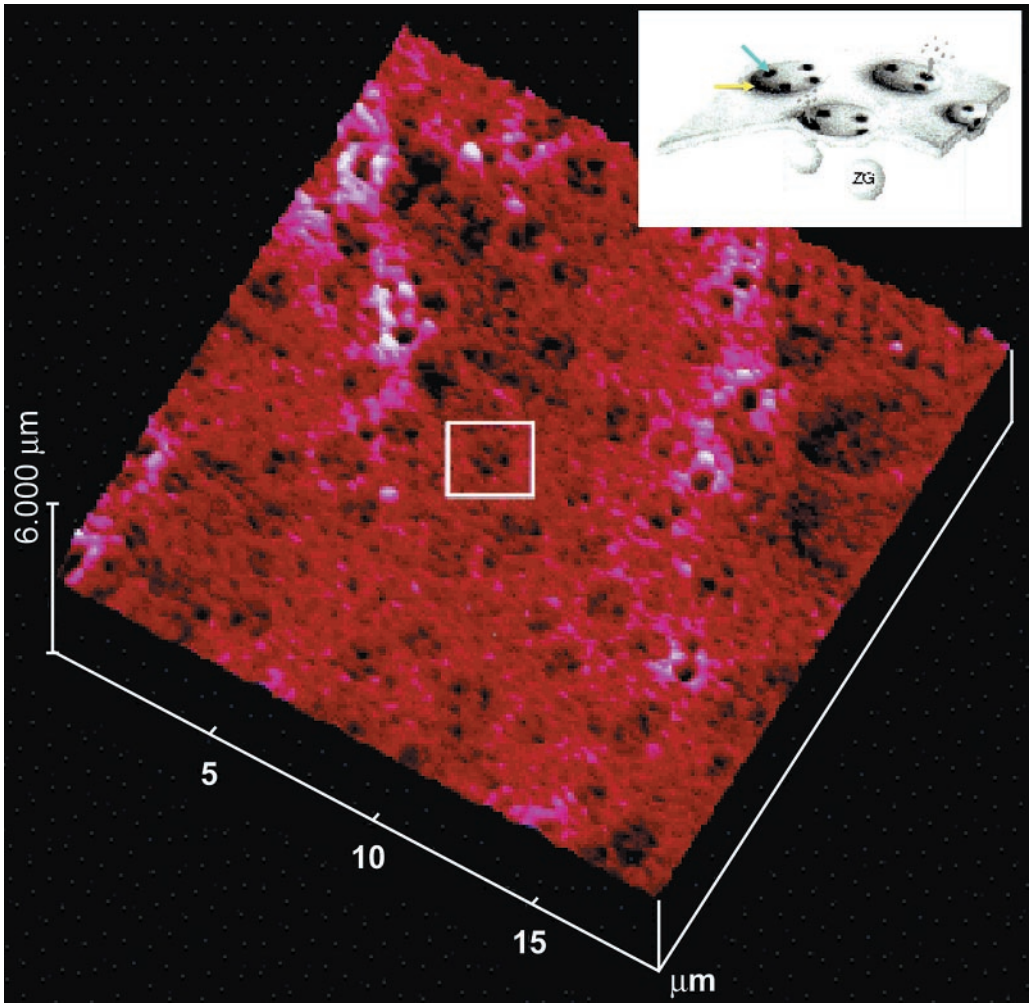

Fig. 2. AFM image of fusion pores at the apical plasma membrane of pancreatic acinar cells. Inset: schematic depiction of secretory vesicle docking and fusion at the fusion pore. Fusion pores or "depressions" (blue arrow), 100 to 180 nm wide and 15 to 25 min in relative depth, are present with "pits" (yellow arrows). ZG, zymogen granule.

However, most biological structures are relatively soft and delicate, and typical imaging forces of tens of nanonewtons can distort or permanently destroy such structures. Recently, two complementary approaches to imposing lower imaging forces have been developed. The first approach is based on increasing the effective quality factor (Q) of an oscillating cantilever in a liquid environment. (Q is the ratio of energy input and energy dissipation in a resonant system; it is also a measure of the sharpness of the resonant peak amplitude.) The second approach involves the development of an entirely new SPM known as photonic force microscopy (PFM).

Increased Force Sensitivity in Liquid

The introduction of the intermittent-contact mode, often referred to as tapping mode, was an important development because it greatly reduced the shear forces on the specimen and, as a dynamic technique, also offered the possibility of phase imaging. At each point in an image, the phase difference between the driving force supplied to the cantilever and the response of the cantilever is related to the interaction between the tip of the probe and the specimen. The relationship between the phase shift and the nature of the tip-specimen interaction is complex; however, images constructed from the phase information are often of practical value in identifying regions of a similar chemical nature.

The tapping mode was initially developed for operation in air, and its eventual application in liquid brought the advantages of the technique to biologically relevant environments. However, oscillation of the cantilever in liquid incurs some disadvantages associated with damping of the can-

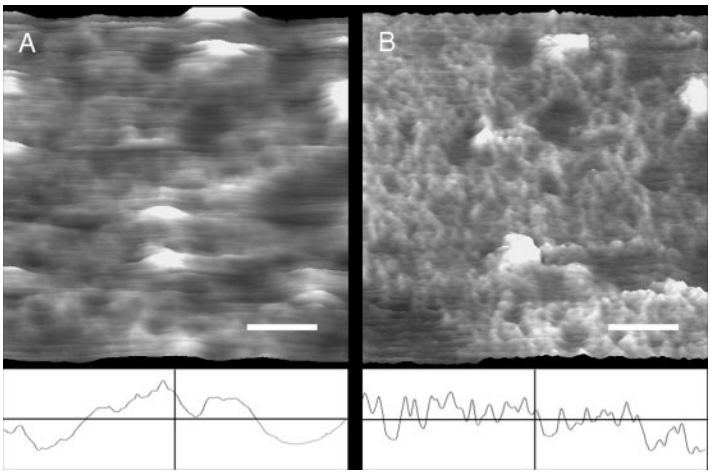

Fig. 3. AFM images of a 30% isotactic polystyrene gel in dekalin (decahydronaphthalene) imaged under dekalin, taken without (**A**) and with (**B**) active-Q feedback. Below each image is a line profile (the variation in height across a horizontal line taken across each image) showing the higher spatial frequencies and thus resolution when the effective Q factor is enhanced. Scale bars, 1 μm; full grayscale, 75 nm.

tilever motion by the liquid. Higher forces are needed to drive the cantilever in liquid, and the damping of the motion results in a decreased Q factor. Thus, the resonant amplitude peak of the cantilever is broadened so that the value of Q ranges from typically a few hundred in air to around 1 in liquid. Sensitivity to the nature of the tip-specimen interaction is greatly reduced, and the phase contrast becomes much weaker.

The recent development of active resonance control when applied to the oscillating cantilever in tapping mode in liquid (*7, 8*) enables an increase in the effective value of the Q factor so that tip-specimen forces are greatly reduced. The higher effective Q value of the cantilever in liquid is achieved by electronically amplifying and phase-shifting the cantilever position information and feeding this back to the cantilever drive transducer in such a manner as to counteract the damping forces of the liquid. The use of this active-resonance (active-Q) technique reduces the deformation of soft biological and organic specimens, resulting in images that have higher resolution or would otherwise be unattainable; the phase contrast in such images is also greatly improved. The application of this technique to the imaging of a gel of polystyrene in dekalin is shown in Fig. 3. The gel was imaged swollen in dekalin in tapping mode. The image in Fig. 3A was obtained without the active-Q mode enabled and shows signs of the AFM tip deforming the gel. An image of the same area of the gel, acquired minutes later with the same tip but with the active-Q feedback enabled (Fig. 3B), shows higher resolution features and essentially no signs of the tip deforming the gel.

AFM in Three Dimensions

Living cells are 3D structures, whereas AFM is a surface tool whose performance is directly coupled to the flatness of the surface investigated. Imaging inside cells is totally impossible because of the instrument's mechanical connection to the imaging tip. Therefore, a scanning probe microscope without a mechanical connection to the tip, working with extremely small loading forces, would be an ideal complementary technique for AFM in studies of live cells. A PFM instrument with these attributes was recently developed at the European Molecular Biology Laboratory (EMBL) in Heidelberg.

For PFM, the mechanical cantilever is replaced by the 3D trapping potential of a laser focus. The possibility of trapping and manipulating micrometer-sized particles (beads) with a laser focused into a fluid chamber was first described by Ashkin in 1986 (*9*), the same year that AFM was introduced. The strength and 3D shape of the trapping potential can be determined from the difference in the refractive index between the bead and the fluid medium, the bead diameter, and the laser intensity and 3D profile. Depending on the application, the trapping potential—which is harmonic and therefore can be described by its spring constant—can be adjusted by changing the laser power. Usually its spring constant is two to three orders of magnitude lower than that of any commercially available AFM cantilevers. The beads used as tips can be as small as ~10 nm in the case of high refractive index materials such as metals. PFM uses a 3D detection system for bead position with respect to trapping potential, allowing measurement of the value and direction of the force acting on the bead with subpiconewton precision on a time scale of microseconds. Beads used as scanning probe tips can be moved along a surface to make interaction force measurements between the tip and the surface in the pico- and subpiconewton force range. If latex or glass beads are used as tips, many standard chemical surface modifications are commercially available; with a bead size of 200 to 400 nm, the objective used to focus the laser provides a good optical control for the measurements.

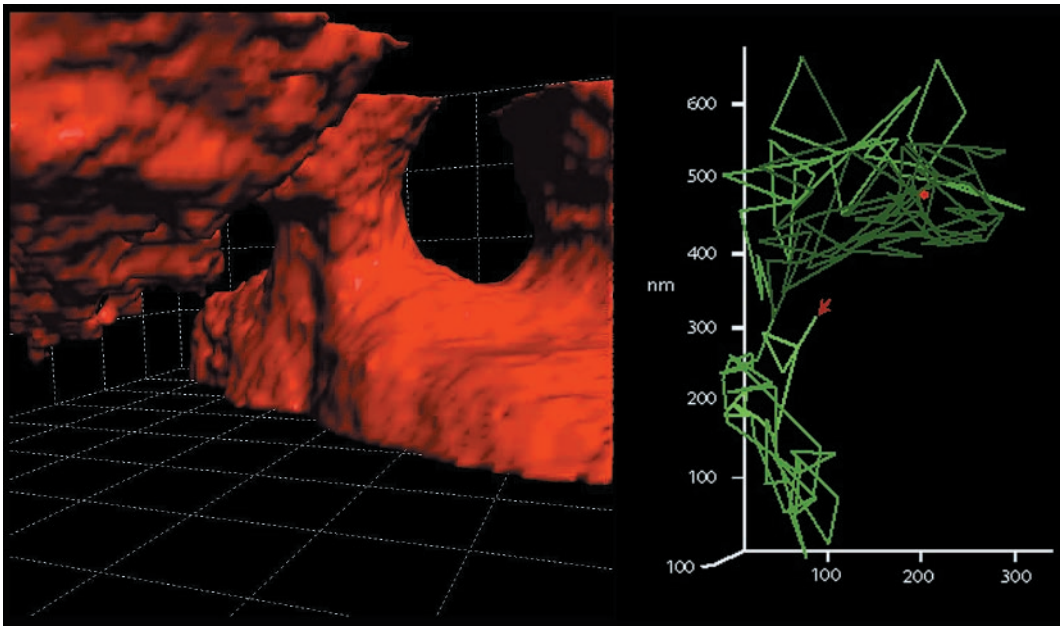

Fig. 4. (**Left**) A 3D thermal noise image of an agar network, showing the volume from which a bead moving under thermal excitation is excluded. (**Right**) The trajectory of a bead trapped in an optical potential well within a gel, from which the local viscoelastic properties can be calculated. The start and latest positions in the trajectory of the particle are indicated by the red dot and arrow, respectively.

The image resolution obtained with these beads by scanning them across a surface while measuring the interaction forces is limited by the interaction area between bead and sample and is also limited by thermal fluctuations, which can be up to 100 nm depending on the trapping potential. With a detection system giving a spatial resolution of better than 1 nm and a time resolution of 1 μs, this limitation can be easily overcome by using the thermal fluctuations as a random scan generator for the exploration (within milliseconds) of a small 3D volume of several tens of nanometers. Such a strategy opens up many new applications because the position probability measured for a certain volume reflects the presence of other objects in this volume, the interaction potential with these objects, and the interaction with the surrounding medium. In this way, 3D polymer networks can be imaged (Fig. 4) (*10*), the mechanical properties of single molecules binding the bead to a surface (*11*) can be measured, and the viscosity of the membrane of living cells in areas smaller than 100 nm in diameter can be measured if beads are linked to single membrane components such as, for example, the LDL (low-density lipoprotein) receptor membrane protein. Such measurements were used to provide evidence for the existence of so-called "membrane raft structures," about 40 nm in diameter, which had long been proposed on the basis of biochemical evidence (*12*).

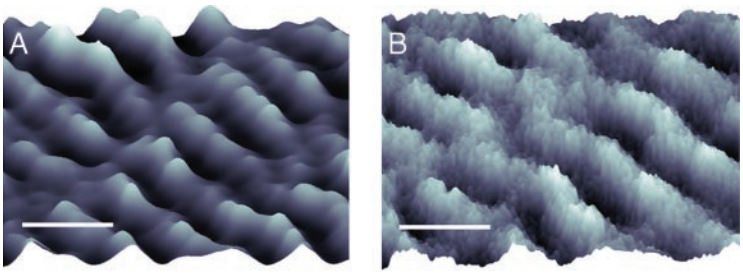

Fig. 5. Near-field scanning optical microscope images of part of a PHB/V [poly(hydroxybutyrate-*co*-hydroxyvalerate)] polymer spherulite showing optical banding. (**A**) Image collected in ~20 min with a conventional scanning system. (**B**) Image collected in 8.3 ms with a high-speed resonant scanning system. Scale bars, 1 μm.

Ultrafast SPM Imaging

Because scanning probe techniques enable control over environmental conditions, they can be used to follow processes in situ, in real time. A good example of this is the new understanding of polymer crystallization that has been gained by temporal resolution of this process (*13*). As the crystallization of an individual lamella is followed in a series of images (*14*), the rate of growth is seen to vary in time for each lamella, as well as from lamella to lamella during the same time period. When following processes, the time resolution of any scanning probe microscope is hindered by the serial nature of the data collection—the very factor that allows the technique to bypass the diffraction limit that applies to conventional microscopes that use lenses. Two factors limit how fast an image can be collected: the response time of the interaction (e.g., of the cantilever in AFM) and the resonant frequency of the scan stage. In the case of AFM, electronic control of the Q factor of the cantilever as described above can be used to reduce the effective Q of the cantilever in air (*15*) and hence reduce its response time; this technique was used to collect the images in movie S1 (*14*). Complementary to this approach, the mechanics of the microscope can be redesigned and optimized for rapid imaging with the use of smaller cantilevers and high–resonant frequency scan stages (*16*). This has pushed the image rate of conventional AFM to ~10 frames/s (*17*), allowing remarkable temporal resolution of the motion of motor proteins.

Recently, the possibility of obtaining SPM images with millisecond resolution has been realized (*18*), giving access to macromolecular relaxation time scales. This new technique uses the resonance of a microscanner to provide the fast scan axis of the image. Each line consists of one resonant sweep of the scanner with an amplitude of several micrometers, using the high stability and well-understood behavior of a resonator to provide the scan system rather than fighting against resonance (as in the conventional approach). The first microscope to use this technique monitors a near-field optical interaction with the sample. Figure 5 shows a near-field optical image of part of a polymer spherulite collected with a conventional SPM in ~20 min and an image collected by the resonant scanning technique in just 8.3 ms.

Microfabricated probes are being developed to increase imaging rates and to lower probe-specimen force interactions. Such probes also allow the combination of different instrument types—for instance, conventional AFM and a scanning electrochemical microscopy (SECM). The integration of an electroactive area at an exactly defined distance above the apex of the atomic force microscope tip allows the distance between electrode and probe to remain constant regardless of the surface topography, which enables simultaneous electrochemical and AFM imaging in tapping mode. Because many biochemically relevant processes are based on electrochemical conversion of molecules, techniques for gathering laterally resolved information on coupled oxidation-reduction processes are of particular interest. As recently shown, the application of such difunctional tips (*19*) allows electrochemical images to also be recorded in AFM tapping mode, which reveals a current response and lateral resolution comparable to the electrochemical images of the same probe recorded in contact mode.

Recent developments in SPM are producing new and fundamental insights across a broad spectrum of scientific disciplines, providing key tools for the emerging fields of nanotechnology and biotechnology. These are exciting times not only for the application of SPM but also for the development of the technique and its ability to answer new questions.

References and Notes

1. G. Binnig, C. F. Quate, C. Gerber, *Phys. Rev. Lett.* **56**, 930 (1986).
2. F. J. Giessibl, *Science* **267**, 68 (1995).
3. W. Häberle, J. K. H. Hörber, F. Ohnesorge, D. P. E. Smith, G. Binnig, *Ultramicroscopy* **42–44**, 1161 (1992).
4. A. A. Baker, W. Helbert, J. Sugiyama, M. J. Miles, *Biophys. J.* **79**, 1139 (2000).
5. S. Scheuring, D. J. Müller, H. Stahlberg, H.-A. Engel, A. Engel, *Eur. Biophys. J.* **31**, 172 (2002).
6. A. Jeremic, M. Kelly, S.-J. Cho, M. H. Stromer, B. P. Jena, *Biophys. J.* **85**, 2035 (2003).
7. J. Tamayo, A. D. L. Humphris, M. J. Miles, *Appl. Phys. Lett.* **77**, 582 (2000).
8. J. Tamayo, A. D. L. Humphris, R. J. Owen, M. J. Miles, *Biophys. J.* **81**, 526 (2001).
9. A. Ashkin, *Opt. Lett.* **11**, 288 (1986).
10. C. Tischer *et al.*, *Appl. Phys. Lett.* **79**, 3878 (2001).
11. S. Jeney, E.-L. Florin, J. K. H. Hörber, in *Kinesin Protocols*, I. Vernos, Ed., vol. 164 of *Methods in Molecular Biology* (Humana, Totowa, NJ, 2000), pp. 91–108.
12. A. Pralle, P. Keller, E.-L. Florin, K. Simons, J. K. H. Hörber, *J. Cell Biol.* **148**, 997 (2000).
13. J. K. Hobbs, A. D. L. Humphris, M. J. Miles, *Macromolecules* **34**, 5508 (2001).
14. Supplementary movies are available on *Science* Online.
15. T. Sulchek *et al.*, *Appl. Phys. Lett.* **76**, 1473 (2000).
16. D. A. Walters *et al.*, *Rev. Sci. Instrum.* **67**, 3583 (1996).
17. T. Ando *et al.*, *Proc. Natl. Acad. Sci. U.S.A.* **98**, 12468 (2001).
18. A. D. L. Humphris, J. K. Hobbs, M. J. Miles, *Appl. Phys. Lett.* **83**, 6 (2003).
19. A. Lugstein, E. Bertagnolli, C. Kranz, A. Kueng, B. Mizaikoff, *Appl. Phys. Lett.* **81**, 349 (2002).
20. The authors thank A. D. L. Humphris, J. K. Hobbs, and T. J. McMaster for valuable discussions during the preparation of this review and A. D. L. Humphris and J. K. Hobbs for their assistance with Movies S1 and S2.

Supporting Online Material

www.sciencemag.org/cgi/content/full/302/5647/1002/DC1

Movies S1 and S2